Observation of direct infrared multiphoton pumping of the triplet manifold of biacetyl

Jeffrey Y. Tsao, Jerry G. Black, and Eli Yablonovitch

Gordon McKay Laboratory, Harvard University, Cambridge, Massachusetts

Itamar Burak

Gordon McKay Labortory and Department of Chemistry, Tel Aviv University, Tel Aviv, Israel
(Received 20 February 1980; accepted 14 May 1980)

Direct collisionless multiphoton (MP) excitation of the triplet vibronic manifold of biacetyl is reported. Following a dye laser pulse which prepares some of the biacetyl molecules in the triplet metastable state, the system is irradiated by an intense 20 ns 9.6μ CO_2 pulse. The CO_2 radiation induces fast quenching of the phosphorescence emission from the ^3A_u excited molecules. It also induces an emission signal in the fluorescence spectral region of biacetyl. This signal is related to an inverse electronic relaxation (IER) from excited triplet vibronic levels into isoenergetic singlet ^1A_u vibronic levels. Analysis of the induced luminescence signals provides information on the collisionless MP prompted vibrational distribution. Excitation with 10.6μ CO_2 pulses leads to the simultaneous MP pumping of both the ground and triplet manifolds. The generation of blue emission signals in this experiment bears a close resemblance to recent observations of prompt visible emission due to MP pumping of ground state molecules. General expressions for the emission intensities are derived with special emphasis on the specific features of MP vibrational distributions. The detectability of MP induced emission signals is discussed.

I. INTRODUCTION

The collisionless, infrared multiphoton excitation of ground state polyatomic molecules has been the subject of many recent investigations. The diagnostics for the multiphoton process have been:

(a) Optoacoustic absorption measurements[1] followed by the determination of the average number of photons absorbed per molecule;

(b) Observation of multiphoton induced chemistry[2];

(c) Observation of infrared induced emission from the excited molecule[3,4] or from excited reaction products.[5]

Infrared multiphoton excitation of the excited electronic states, however, is still a new research area. In this case, changes in the luminescence are expected to be induced by the vibrational excitation, and thus a powerful new diagnostic is added to the investigation of the infrared multiphoton processes. For example, the collisionless multiphoton pumping of electronically excited NO_2 molecules has recently been reported,[6] in which an analysis of the induced changes in the emission spectra provided an estimation for the n-photon absorption probability $P(n)$.

In this work we report the direct infrared excitation of the triplet state of biacetyl. First, a dye laser pulse pumps the ground state into the ^1A_u first excited singlet state (see Fig. 1), from which intramolecular couplings between the vibronic manifolds of the ^1A_u and ^3A_u electronic states and collision-induced vibrational relaxation lead to the trapping of some of the excited molecules in the metastable triplet state.[7] This state is characterized by a green phosphorescence which originates from a weakly allowed radiative transition to the ground state. Its decay is dominated by a radiationless transition to the ^1A_g ground state, and at room temperature is 1.7 ms as measured from the phosphorescence lifetime.[8] (This value should be compared with the radiative lifetime of 12 msec.[7])

Then, irradiation of the optically excited biacetyl sample with an intense infrared CO_2 laser pulse leads to the excitation of the triplet vibrational manifold. This excitation is characterized by a prompt burst of blue fluorescence, and a fast partial quenching of the green phosphorescence emission. These effects, first observed by Burak, Quelly, and Steinfeld[9] (BQS), have been interpreted as follows. Due to the intramolecular scrambling of the ^1A_u and ^3A_u zeroth order Born–Oppenheimer vibrational manifolds, a new vibronic manifold is formed. The vibronic levels of this manifold are described as a mixture of singlet and triplet vibronic states and consequently carry oscillator strength for emission in both the fluorescence and phosphorescence spectral regions. The observed blue fluorescence signal is due to the CO_2 laser induced accessibility of vibronic levels

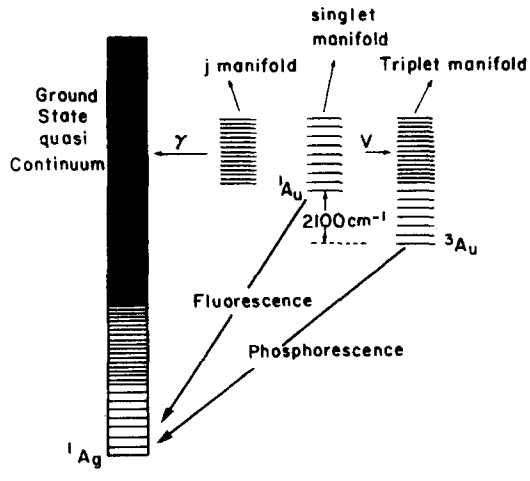

FIG. 1. A schematic diagram of the vibronic manifolds of biacetyl.

 0021-9606/80/172076-08$01.00

with vibrational energy exceeding the singlet–triplet separation energy, and therefore with partly singlet character. The fast drop in the phosphorescence intensity induced by the CO_2 laser is due to the increase, with vibrational energy, in the radiationless transition rate to the ground state. The dependence of this radiationless transition rate $\gamma(E)$ on vibrational energy E has been measured by Van der Werf and Kommandeur.[7]

The previous experiments by BQS[9] involved mainly the indirect vibrational excitation of the triplet manifold. They used 10.6 μ CO_2 laser radiation which preferentially excited the ground rather than the triplet electronic state. The hot ^1A_g molecules then acted as a heat bath for the thermalization of those molecules in the triplet state, thereby increasing the observed phosphorescence decay rate. The present work, using both 9.6 μ, which preferentially excites the triplet over the ground electronic state, and 10.6 μ CO_2 laser radiation, presents evidence for the direct multiphoton pumping of the triplet state. In order to detect an initial nonthermal vibrational distribution, the BQS experiment has been modified. Better time resolution was achieved by shortening the width of the CO_2 laser pulse from 100 to 20 nsec. The use of a more intense, pulsed dye laser instead of a cw argon ion laser provided detectable visible signals from low pressure biacetyl samples. Thus, the lowest pressure in the present experiment was 50 mTorr, while in the former experiment it was 5 Torr. A detailed description of the experimental system is contained in Sec. III. A summary of the theoretical background involving the structure of the mixed singlet–triplet vibrational manifold is presented in Sec. II. The experimental results are summarized and discussed in Secs. IV and V, respectively. In the last section our results will be generalized to the case of light emission due to multiphoton pumping to vibrational levels isoenergetic with the vibronic manifold of an optically active excited electronic state. This case includes the recently observed CO_2 induced emission from CrO_2Cl_2[3] and F_2CO.[4] The theoretical aspects of these inverse electronic relaxation (IER) phenomena have been discussed by Jortner and Nitzan.[10,11] In Sec. VI the IER theory will be used to provide some criteria for the experimental detectability of IER induced emission.

II. THEORETICAL AND EXPERIMENTAL BACKGROUND

The photophysics of biacetyl has been discussed in detail elsewhere.[7,12] The intramolecular interactions between the zero order Born–Oppenheimer singlet and triplet vibronic levels lead to the formation of a single manifold; the $|j\rangle$ levels of this manifold are mixtures of the zero order singlet and triplet states. It is convenient to divide the $|j\rangle$ manifold into vibrational energy regions A and B. Region A is characterized by a low density of zero order singlet vibronic levels. It includes the pure unmixed triplet vibronic states with vibrational energy below E_{ST}, the singlet triplet separation energy. Above E_{ST} each singlet vibronic level $|Si\rangle$ interacts with a set of triplet vibronic levels confined to a width Δ_{ST} around E_{Si}, where

$$\Delta_{ST} = 2\pi v^2 \rho_T \,. \tag{1}$$

v is the mean singlet triplet interaction energy and ρ_T the mean triplet vibronic density. Diagonalization of the molecular Hamiltonian of this set leads to the formation of new wave functions which are admixtures of the $|Si\rangle$ state with the interacting set of triplet vibronic levels. Consequently the A region is divided into "black hole" and "contaminated" subregions. The contaminated subregions consist of mixed vibronic levels, and are confined to strips of width Δ_{ST} around the vibrational energy E_{Si} of the singlet states $|Si\rangle$. The black hole subregions consist of pure triplet vibronic levels, and lie between the contaminated subregions. Region B is characterized by overlapping singlet vibronic levels. More precisely, region B starts at vibrational energies where the homogeneous widths of the singlet vibronic levels $|Si\rangle$ exceed ρ_S^{-1}, the mean separation between adjacent singlet levels. All states in region B are therefore contaminated with one or more zero order singlet states.

Each level $|j\rangle$ in the diagonalized manifold has a width $\gamma_j(E)$ which is the sum of a radiative width γ_j^{rad}, and a nonradiative width γ_j^{nr}, due to irreversible decay into the dense ground state vibronic manifold. Since the nonradiative width dominates over the whole $|j\rangle$ manifold, $\gamma_j(E) \sim \gamma_j^{nr}(E)$. Relations between γ_j and the zero order singlet and triplet level widths γ_S and γ_T have been derived for the two regions.[12] In region A:

$$\gamma_j^A(E) = \gamma_T(E) + \frac{\sum_S \theta(E - E_S)\gamma_S(E_S)}{N_A(E)} \,. \tag{2}$$

The singlet character of the level E_S is diluted by the mean number N_A of interacting triplet vibronic levels, where

$$N_A(E) = \Delta_{ST}\rho_T(E) \,. \tag{2a}$$

$\theta(E - E_S)$ is a step function defined as

$$\theta(E - E_S) = \begin{cases} 1 & -\tfrac{1}{2}\Delta_{ST} < E_S < \tfrac{1}{2}\Delta_{ST} \\ 0 & \text{elsewhere} \end{cases} \,. \tag{2b}$$

In region B:

$$\gamma_j^B(E) = \gamma_T(E) + \frac{\gamma_S(E)}{N_B(E)} \,, \tag{3}$$

where $N_B(E)$ is given by

$$N_B(E) = \frac{\rho_T(E)}{\rho_S(E)} \,. \tag{3a}$$

The emission, due to the presence of zero order singlet–triplet oscillator strengths in the contaminated $|j\rangle$ levels, will be in both the fluorescence and phosphorescence spectral regions, and will have of course the same decay rate in both spectral regions.

These decay rates have been measured in experiments carried out by Van der Werf and Kommandeur.[7] In their experiments, a dye laser was used to optically prepare a state characterized by a zero order singlet vibronic wave function $|Si\rangle$. This $|Si\rangle$ state is a superposition of $|j\rangle$ eigenstates

$$|\Psi(0)\rangle = |Si\rangle = \sum C_j |j\rangle \,, \tag{4}$$

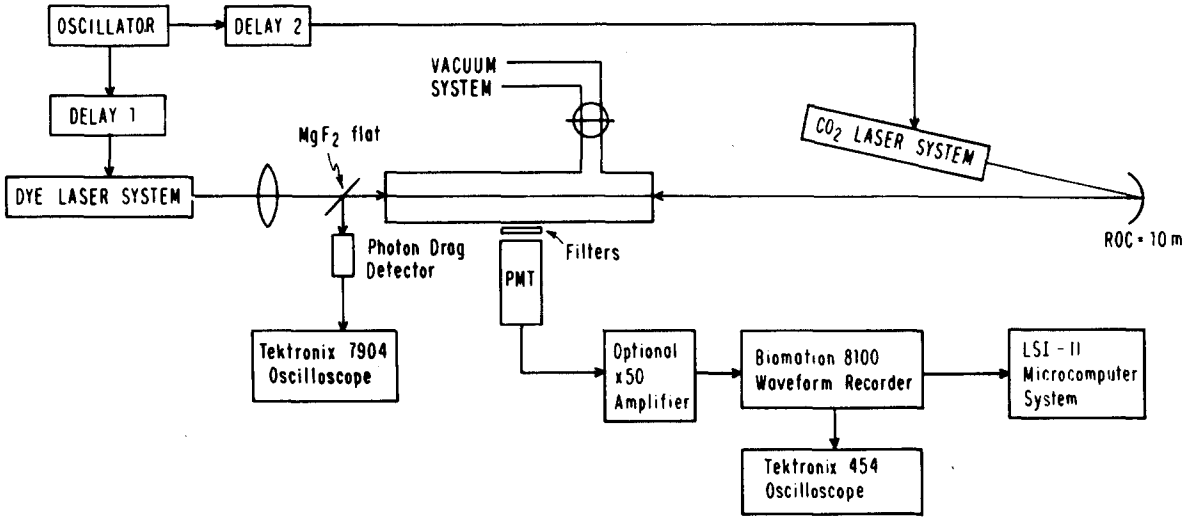

FIG. 2. A schematic diagram of the experimental system.

with a time evolution given by

$$|\Psi(t)\rangle = \sum_j C_j \exp(-iE_j t/h) \exp(-\gamma_j t/2) |j\rangle \ . \qquad (5)$$

The decay of the luminescence emission probability is determined by the quantity $|\langle S|\Psi(t)\rangle|^2$. Lahmani *et al.*[13] have shown that this decay can be expressed as a sum of coherent and incoherent contributions, approximated by a biexponential decay. The fast component is due to the dephasing of the initially prepared superposition, while the long component is a superposition of the independent decays of the excited j levels, and therefore described by the mean decay rates in Eqs. (2) and (3). The dependence of these $\gamma(E)$ on vibrational energy was then determined by measuring the long component of the fluorescence under collisionless conditions, and found to increase steadily with vibrational energy.

III. EXPERIMENTAL

A schematic diagram of the experimental system is shown in Fig. 2. Biacetyl (purchased from Aldrich Chemical Company, 99% purity) was, after freeze–pump–thaw distillations, transferred to a 5 cm diam, 39 cm long Pyrex luminescence cell with NaCl windows at each end. The cell was irradiated in one direction by 20 ns, 20 μJ dye laser pulses whose pump source was a frequency doubled, Q-switched ruby laser. The wavelengths used were in the range of 405–450 nm, and the focused spot diameter was 1 mm. Counterpropagating through the cell in the other direction was a 20 ns, 0.6 J, "truncated" CO_2 laser pulse. The time interval between the two pulses was adjustable up to a jitter of 60 ns determined by the firing of the CO_2 laser.

The CO_2 laser pulse was derived from a Tachisto 215 oscillator–plasma shutter–Lumonics TEA 103-1 amplifier system. For a detailed description of the laser system, see Ref. 14. The oscillator output was, via a 1 inch focal length germanium lens, brought to a focus next to an aluminum block onto which a small fraction of the pulse was diverted. The UV radiation caused by the spark on the aluminum block was sufficient to precipitate an avalanche breakdown within the focal region of the main pulse, creating an overdense plasma, and truncating the CO_2 pulse. A 20 ns FWHM pulse with no tail is thereby generated from a 100 ns pulse with a long tail. The shape of the truncated pulse is shown in Fig. 3. The resulting pulse is then amplified, and focused by a 10 m radius of curvature mirror to a 3 mm spot diameter into the luminescence cell. The overlap cross section between the two laser pulses was therefore confined to the central, more uniform part of the CO_2 beam. A MgF_2 flat served the dual purpose of diverting part of the CO_2 beam to a photon drag detector, and preventing damage to the dye laser's glass optics.

The induced luminescence was monitored perpendicular to the excitation beam using either a Hamamatsu R712, or an EMI 9635QB photomultiplier tube, depending on the spectral region, in conjunction with appropriate interference filters. If the signals were weak, they were first passed through an 8 ns FWHM, gain of 50 homebuilt amplifier (consisting of an LM733 video amplifier and an LH033 buffer) before being recorded by a Biomation 8100 Waveform Recorder. The total system response time was, including laser jitter, 80 ns FWHM. After each shot, the data stored in the Biomation was read into a home-assembled Digitial Equipment Corpora-

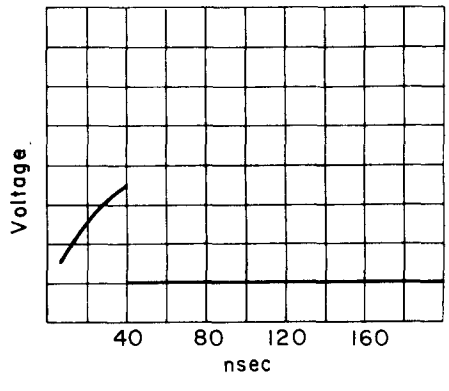

FIG. 3. The truncated CO_2 pulse. Time scale 20 ns/div.

tion LSI-11 microcomputer, and averaged with previous shots.

IV. RESULTS

In this section, the infrared laser induced changes in the characteristic luminescence from the triplet manifold of biacetyl will be described. Biacetyl samples were excited with a pulsed dye laser tuned to 405 nm, and a CO_2 laser fired at a controlled delay following the excitation by the optical pulse. Luminescence was observed in two spectral regions. A narrow band filter centered at 470 nm was used to monitor the blue spectral region; these signals will henceforth be referred to as the fluorescence signals. A long pass filter with a cutoff at 500 nm was used to monitor the phosphorescence; these signals will henceforth be referred to as the phosphorescence signals.

Figure 4 shows the infrared absorption spectrum of biacetyl between 900 and 1200 cm^{-1}. One of the absorption peaks overlaps the CO_2 10.6 μ P branch, but none overlap the 9.6 μ P branch. The CO_2 laser was tuned to the $P(20)$ transitions of both the 9.6 and 10.6 μ bands.

A. 9.6 μ excitation

The effects of the 9.6 μ CO_2 radiation on the phosphorescence signal are exhibited in Fig. 5(a). The optical pulse induces a phosphorescence signal. In the absence of CO_2 radiation, the phosphorescence decays rapidly (on a μs scale) to a quasistationary value, after which it decays slowly with a characteristic lifetime of 1.7 msec. When the phosphorescence intensity attains its quasistationary value, the CO_2 laser is fired. Exposure of the excited system to CO_2 radiation induces a fast decay of the phosphorescence signal from a value I_0 to a value I on a time scale much shorter than the characteristic decay time of the unperturbed phosphorescence. Two main decay components are identified: a fast, pressure independent component with a decay rate greater than 10^7 sec^{-1}, and a slower component, the lifetime of which varies inversely with pressure. Attenuation of the CO_2 pulse results in a smaller drop in the phosphorescence intensity. In order to characterize the drop quantitatively, a yield Y_D, is defined as

$$Y_D = 1 - (I/I_0) \ . \tag{6}$$

The drop yield corresponding to a CO_2 fluence of 4.0 J/cm^2 is 0.7. Attenuation of the CO_2 pulse by a factor of two reduces the drop to 0.15, and leads also to the disappearance of the fast component. A lower value is obtained for the drop yield if it is confined to the fast component; a fast drop yield Y_D^f is defined through

$$Y_D^f = 1 - (I_f/I_0) \ , \tag{7}$$

where I_f is the phosphorescence intensity following the fast decay. Thus a value of 0.4 is obtained for Y_D^f at a fluence of 4.0 J/cm^2. The fast drop yield is increased if the delay time between the optical and the CO_2 pulse is decreased. Figure 6 shows the fast drop yield as a function of the delay between the two pulses. As the delay is increased, Y_D^f decreases exponentially toward a steady value, at a rate which increases linearly with pressure, and with a value of 3.3×10^6 s^{-1} $Torr^{-1}$.

The induced fluorescence signal [Fig. 5(b)] is characterized by an instantaneous, pressure independent rise

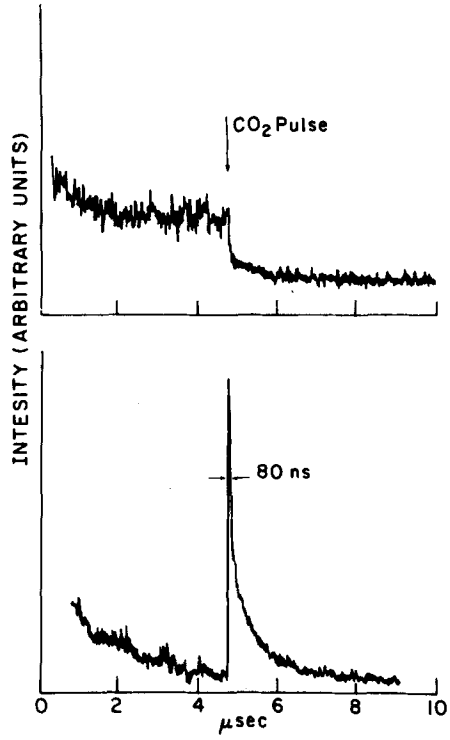

FIG. 5. 9.6 μ induced emission signals. Upper (a) and bottom (b) traces correspond to the phosphorescence and fluorescence emission signals, respectively. The zero time corresponds to the optical excitation, by the dye laser pulse. The introduction of the IR pulse is indicated by an arrow.

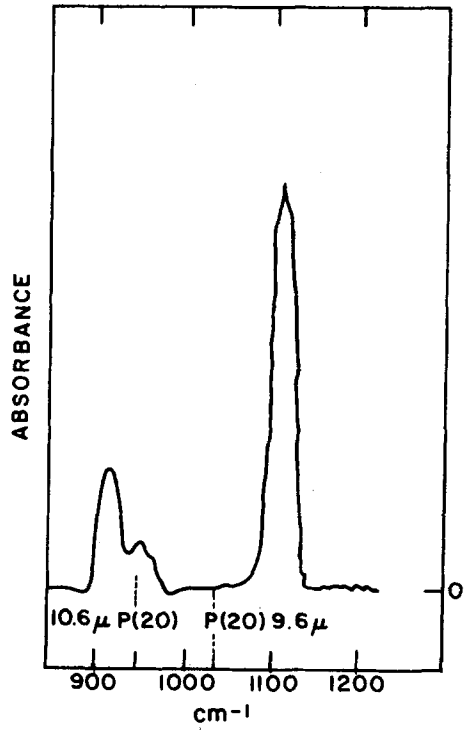

FIG. 4. IR absorbance spectrum of biacetyl.

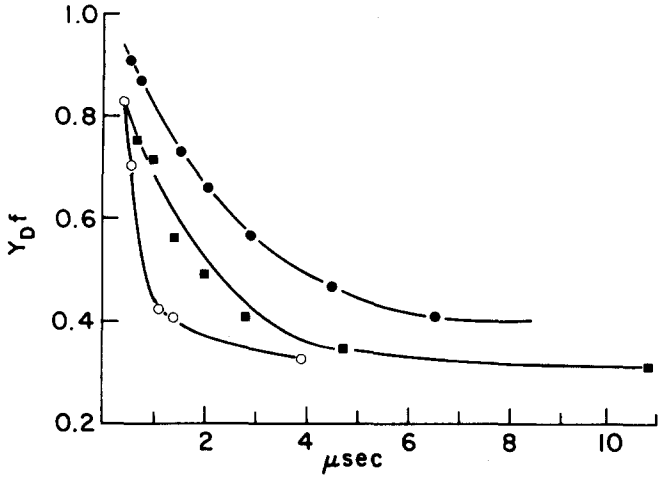

FIG. 6. Y_D^f vs the delay between the visible and IR pulses for various pressures of biacetyl. ● 150 mTorr, ■ 250 mTorr, 500 mTorr.

time, and a decay similar to that observed for the induced phosphorescence signal. The decay times of the long components of the fluorescence and phosphorescence signal exhibit the same $P\tau$ relations. A plot of τ^{-1} vs pressure is shown in Fig. 7; a value of 4×10^6 s^{-1} $Torr^{-1}$ is obtained for the collisional decay rate.

B. 10.6 μ induced signals

Similar to the 9.6 μ case, irradiation with 10.6 μ CO_2 pulses results in a prompt induced fluorescence and a phosphorescence quenching. The rise time of the fluorescence signal is instantaneous and pressure independent. The decays of the 10.6 μ induced signals, however, are characterized by the appearance of a new component whose lifetime depends strongly on the CO_2 laser fluence. Figure 8 shows two typical fluorescence signals, corresponding to high and low fluence. The signals are characterized by an initial spike followed by a longer decay component whose lifetime decreases as the fluence increases. The phosphorescence has the same longer decay component behavior as the fluorescence, but lacks the fast initial decay seen in the 9.6 μ case.

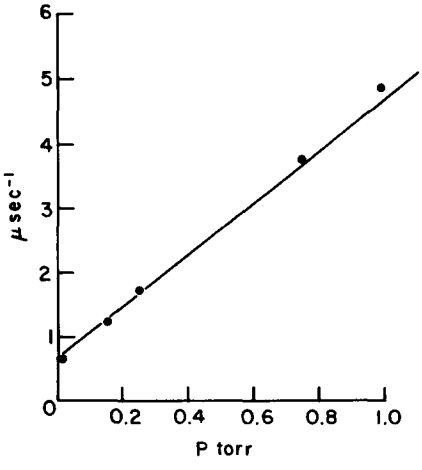

FIG. 7. Quenching rates of the slow component of the 9.6 μ induced fluorescence signal vs the pressure of the biacetyl.

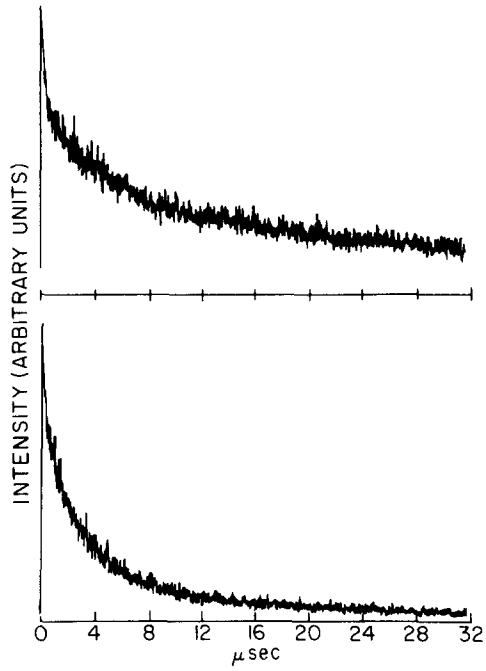

FIG. 8. 10.6 μ induced fluorescence signals from 1 Torr biacetyl sample. The lower trace is prompted by 5.0 J/cm^2 CO_2 pulse. The upper trace is induced by 2.5 J/cm^2 CO_2 pulse.

V. DISCUSSION

The induced fluorescence and phosphorescence signals reported in the last sections indicate a vibrational excitation within the triplet manifold. The absence of pressure effects on the rise time of the induced fluorescence signals excludes collisional causes; moreover, the short, 20 ns width of the CO_2 pulse ensures a collisionless excitation process. Since the triplet–singlet electronic separation energy is 2100 cm^{-1}, the generation of a blue fluorescence signal sets a lower limit to the accessed vibrational energy of two CO_2 photons.

As a result of the collisionless multiphoton process a nonthermal distribution is established within the triplet manifold. Subsequent changes in the populations of the initially excited vibronic levels are controlled by two mechanisms:

1. An intramolecular conversion into the ground electronic state depletes the population of the excited electronically state. If $n(E)$ is the population density of triplet molecules with vibrational energy E, the depletion rate of this level is given by

$$\frac{d}{dt}n(E) = -\gamma(E)n(E) \ . \tag{8}$$

The intramolecular depletion of the total number of electronically excited molecules N_T is given by

$$\frac{dN_T}{dt} = -\int\gamma(E)n(E)\,dE \ . \tag{9}$$

2. Vibrational relaxation processes due to collisions with ground state molecules lead to vibrational energy redistribution. Ultimately, equilibration between the vibrational temperatures of the ground and triplet electronic states is established.

The fast, pressure independent component of the 9.6 μ induced emission signals is due to the intramolecular decay of molecules excited to high vibrational levels, where radiationless transitions to the ground state are extremely fast. If k is the collisional relaxation rate of molecules excited to vibrational energy E, then the fast component originates from molecules whose vibrational energy exceeds E_f, where E_f is defined by

$$\gamma(E_f) = k \ . \tag{10}$$

The pressure controlled component of the 9.6 μ induced emission signals is due to emission from vibronic levels whose intramolecular decay time is comparable to or longer than the thermalization time τ_{th}. The latter quantity is the characteristic time needed to collisionally relax the vibrational excitation to a room temperature vibrational distribution. In addition, the dependence of Y_D^f on the delay between the dye and CO_2 laser pulses is also due to collisional relaxation. The optical laser pulse prepares a narrow distribution of triplet molecules around the vibrational energy E. When the CO_2 pulse is applied, the optically prepared excited molecules are pumped to vibrational energy regions where the intramolecular decay process dominates. The almost unity value of Y_D^f for zero delay times indicates that all the optically prepared molecules have been pumped by the CO_2 pulse to the fast decaying energy region. As the optically prepared vibrational distribution cools, the CO_2 pulse is able to excite fewer molecules to the fast decaying energy region. Finally, the yield reaches a steady value which does not change with further increase of the delay time; this value of Y_D^f corresponds to excitation of the thermalized triplet state. Therefore, both the 4.1×10^6 s^{-1} $Torr^{-1}$ collisional quenching rate of the induced fluorescence signal and the 3.3×10^6 s^{-1} $Torr^{-1}$ decay rate of the fast drop yield Y_D^f are estimates of the collisional thermalization of the excited vibrational distribution.

Since vibrational excitation is maintained only through the thermalization time τ_{th}, intramolecular radiationless decay is confined to triplet molecules occupying vibronic levels with energy E greater than E_l, where

$$\gamma(E_l) = \tau_{th}^{-1} \ . \tag{11}$$

The determination of Y_D and E_l provides information about the initial vibrational distribution in the following way. Y_D is the fraction of molecules excited to vibrational energies exceeding E_l. 9.6 μ CO_2 pulses with fluence 3.3 J/cm^2 induce phosphorescence signals characterized by a drop yield of 0.65. The thermalization time corresponding to 150 mTorr biacetyl samples is about 1 μs; using the data reported by Van der Werf and Kommandeur, a radiationless decay time of 1 μs corresponds to a vibrational energy of 5400 cm^{-1}. Since Y_D is the fraction of molecules excited to vibrational energies exceeding E_l, 65% of the triplet molecules were excited to vibrational energies exceeding that of 5 CO_2 photons. Another lower limit is obtained by using the fast drop yield $Y_D^f = 0.4$. The fast, 100 ns decay time corresponds to an energy of 9 CO_2 photons; thus a fraction 0.4 of the triplet molecules have absorbed more than 9 CO_2 photons. (Since the decay times reported in Ref. 7 were limited to times longer than 300 ns, we extrapolated $\gamma(E)$ using the following approximation[12]:

$$\gamma(E) = A\, e^{BE} + C \ , \tag{12}$$

where $A = 300$ s^{-1}, $B = 1.26\times10^{-3}$ cm, and $C = 82$ s^{-1}.)

Information concerning the 10.6 μ direct MP vibrational excitation is limited due to the appearance of a thermal component. The dependence of the decay time of this component on the fluence of the CO_2 laser has been extensively explored and accounted for by Burak *et al.*[9] The ground electronic state of biacetyl strongly absorbs the 10.6 μ radiation; the average number of photons absorbed per molecule $\langle n\rangle$ determines the rapidly established temperature of the ground state vibrational manifold through

$$\langle n\rangle \cdot h\nu_{CO_2} = \langle E_0\rangle + \left(\int_0^\infty \rho(E) E\, e^{-E/kT}\, dE \Big/ \int_0^\infty \rho(E)\, e^{-E/kT}\right) , \tag{13}$$

where E_0 is the mean energy of unexcited biacetyl molecules. Since biacetyl molecules in the ground state constitute the major component in the triplet–ground state mixture, they may be regarded as a heat bath. When a thermal quasiequilibrium between the two vibronic manifolds is established the triplet molecules will decay with a thermalized rate constant $\langle\gamma\rangle$:

$$\langle\gamma\rangle = \left(\int_0^\infty \gamma(E)\rho(E)\, e^{-E/kT} dE \Big/ \int_0^\infty \rho(E)\, e^{-E/kT} dE\right) , \tag{14}$$

$$dN_T/dt = -\langle\gamma\rangle N_T \ . \tag{15}$$

An increase in the fluence will result in more photons absorbed, a higher heat bath temperature, and an increased decay rate $\langle\gamma\rangle$.

The instantaneous rise time of the 10.6 μ induced fluorescence signal does indicate some direct infrared excitation of the triplet state, in addition to that of the ground state. The overall transient behavior of the 10.6 μ signals is therefore determined by the following sequence of events. The CO_2 laser excites both the triplet and ground electronic states. While ground state molecules relax to a thermal distribution, the initial nonthermal triplet vibrational distribution relaxes towards the vibrational temperature of the heat bath. When a thermalization is achieved in a time τ_{th}, the residual triplet molecules which have not yet undergone a radiationless transition will decay with the thermalized rate $\langle\gamma\rangle$. The efficiency of the 10.6 μ radiation at directly pumping the triplet state is considerably less than that of the 9.6 μ radiation. The fast, pressure independent decay component of the 9.6 μ induced signals is *not* observed for the 10.6 μ signals, indicating that a negligible fraction of triplet molecules is excited to the vibrational region where the condition $\gamma(E) > k$, is fulfilled. The enhanced efficiency of the 9.6 multiphoton excitation might be related to the red shifting of the ground state IR vibrational spectrum in the triplet state of biacetyl. The relevant ground state spectrum (shown in Fig. 3) consists of the following three bands[15]:

1. A strong absorption band centered at 1115 cm^{-1} assigned to the CH_3 a_u or b_u rocking mode.

2. A 945 cm^{-1}, medium strength absorption band related to the C–CH_3 b_u stretching mode.

3. A 915 cm^{-1} medium strength combination band due to the 539 cm^{-1} and 380 cm^{-1} b_u and a_g bending modes, respectively.

A partial analysis of the vibrational modes of the triplet electronic states has been carried out by Sidman and McClure.[15] The frequencies of some of the analyzed modes are red shifted with respect to the corresponding ground state modes. It is therefore conceivable that the 1045 cm^{-1} $P(20)$ 9.6 μ transaction coincides with the frequency of the strongly absorbing CH_3 rocking mode.

VI. MULTIPHOTON INDUCED IER PROCESS

The generation of induced blue fluorescence emission reported in this manuscript bears a close resemblance to the observation of induced visible emission due to the multiphoton excitation of ground state molecules. Emission induced by high fluence CO_2 pulses has been observed from excited CrO_2Cl_2[3] and F_2CO[4] samples. Jortner and Nitzan[10] and Burak *et al.*[9] have explained the CrO_2Cl_2 emission as originating from multiphoton excitation to vibrational energy regions where the ground state manifold is scarmbled with vibronic levels of an excited electronic state. Jortner and Nitzan have carried out an extensive theoretical study of the inverse electronic relaxation (IER) process leading to the observed emission. Karny *et al.*[3] rejected the IER mechanism in CrO_2Cl_2 on the basis that the ground state density at the origin of the electronic excited state is too high to provide a reversible conversion, suggesting instead the possibility of direct infrared transitions from high vibrational levels of the ground state and low vibronic levels of the excited electronic state.

In this section we shall apply the IER theory to obtain criteria for the experimental detectability of multiphoton induced IER processes. Our treatment will be confined to a $|j\rangle$ vibronic manifold resulting from the scrambling of an excited electronic vibronic manifold $|S\beta\rangle$ with isoenergetic vibronic levels $|G\alpha\rangle$ of the ground electronic state. The width of the $|j\rangle$ levels may be constructed from the zero order widths of the $|G\alpha\rangle$ and $|S\beta\rangle$ states by equations which are similar to Eqs. (2) and (3). Again, the scrambled manifold is divided into regions A and B corresponding to low and high vibrational densities, respectively, of the zero order $|S\beta\rangle$ states. The widths of the $|j\rangle$ levels in region A are given by[10,11]

$$\gamma_j^A(E)=\frac{\gamma_S\theta(E-E_{S\beta})}{N_A(E)}\,, \tag{16a}$$

$$N_A(E)=2\pi v^2\rho_G(E)\,. \tag{16b}$$

In region B the widths are given by

$$\gamma_j^B(E)=\frac{\gamma_S}{N_B(E)} \tag{17}$$

$$N_B(E)=\frac{\rho_G(E)}{\rho_S(E)}\,. \tag{17a}$$

In contrast to the radiationless decay widths given in Eqs. (2) and (3), the widths γ_j and γ_S in Eqs. (17) and (18) are radiative decay widths. The zero order width γ_S is diluted by the factors N_A or N_B.

Following the collisionless multiphoton process a nonthermal vibrational distribution is established within the $|j\rangle$ manifold. The distribution is characterized by excitation strips of width ΔP_n around the energies E_n, where

$$E_n=nh\nu_{CO_2}\,,\qquad n=0,1,2,3,\ldots\,, \tag{18}$$

and ΔP_n is a power broadening width. These excitation strips are populated by the multiphoton process with probabilities $p(n)$.

The rate of photon emission I is the sum of the rates I_A and I_B contributed by molecules excited to regions A and B respectively. To calculate I_A it is convenient to subdivide region A into regions $A_{\rm I}$ and $A_{\rm II}$. $A_{\rm I}$ is the energy region of extremely spare density of $|S\rangle$ levels, *viz.*, $\Delta P_n\rho_S<1$. Region $A_{\rm II}$ is characterized by $\Delta P_n\rho_S>1$. Both regions $A_{\rm I}$ and $A_{\rm II}$ are of course characterized by $\Delta_{SG}\rho_S<1$. The emission rate from region $A_{\rm I}$, $I_{A_{\rm I}}$, is given by

$$I_{A_{\rm I}}=N_0\gamma_S\sum_{\kappa_0}^{\kappa'}\frac{f(n)}{N_A(E)}p(n)\theta'(E_n-E_{Si})\,, \tag{19}$$

where κ_0 is the lowest integer fulfilling $\kappa_0\hbar\omega_{CO_2}>E_{SG}$, $\kappa'\hbar\omega_{CO_2}$ is the boundary between regions $A_{\rm I}$ and $A_{\rm II}$, E_{SG} is the separation energy of the G and S origins, and N_0 is the number of molecules in the laser field. $\gamma_S/N_A(E_n)$ is the diluted emission rate from the contaminated $|j\rangle$ levels excited to the nth subregion. $f(n)$ is the fraction of molecules within the nth subregion which are contaminated. $\theta'(E-E_{Si})$ is defined through Eq. (2b), except that the homogeneous width Δ_{ST} is replaced by the power broadening width ΔP_n. The introduction of the step function $\theta'(E)$ emphasizes the need for exact resonances in the $A_{\rm I}$ region: unless there exists an S level within the range Δp_n around E_n, there can be no emissions from the excitation strip around E_n.

In region $A_{\rm II}$ on the other hand, all the excitation strips contribute to the emission. The number of contaminated states within the excited nth region is $\Delta P_n\rho_S$, and therefore

$$I_{A_{\rm II}}=N_0\gamma_S\sum_{\kappa'}^{\kappa_{AB}}\frac{f(n)}{N_A(E)}p(n)\Delta P_n\rho_S\,, \tag{20}$$

where $\kappa_{AB}\hbar\omega_{CO_2}$ is the boundary between regions A and B, and f_n is estimated as

$$f_n=\Delta_{SG}/\Delta P_n\,. \tag{21}$$

Substituting (21) for f_n and $\Delta_{SG}\rho_G$ for N_A in Eq. (20) results in

$$I_{A_{\rm II}}=N_0\gamma_S\sum_{\kappa'}^{\kappa_{AB}}\frac{\rho_S}{\rho_G}p(n)\,. \tag{22}$$

In contrast to the MP excitation in region A, each excitation strip in region B contributes to light emission. Since all the $|j\rangle$ levels in this region are contaminated, $f(n)=1$. The rate of photon emission I_B is given by

$$I_B=\gamma_S N_0\sum_{\kappa_{AB}}^{\infty}\frac{p(n)}{N_B(E)}=\gamma_S N_0\sum_{\kappa_{AB}}^{\infty}\frac{\rho_S}{\rho_G}p(n)\ . \tag{23}$$

If accidental resonances in region A_{I} are neglected, the sum rate of photon emission will be given by

$$I=I_{A_{\mathrm{II}}}+I_B=\gamma_S N_0\sum_{\kappa'}^{\infty}\frac{\rho_S}{\rho_G}p(n)\ . \tag{24}$$

Since ρ_S/ρ_G is a slowly increasing function of the vibrational energy E,[11] a lower bound $\bar{I}$ may be obtained for the photon emission rate from

$$\bar{I}=\gamma_S N_0\left(\frac{\rho_S}{\rho_G}\right)_0\sum_{n=\kappa'}^{\infty}p(n)\ , \tag{25}$$

where $[(\rho_S)/\rho_G]_0$ is the density of states ratio at the origin of the excited S state. Equation (25) can be used to estimate the plausibility of detecting emission due to a multiphoton induced IER process. We shall assume that the experiment is limited to detecting photons at a rate faster than 1 photon per μs. Assuming $N_0=10^{13}$ and taking the CrO_2Cl_2 molecule values of γ_S^{rad} and $[(\rho_S)/\rho_G]_0$ as $10^6\ \mathrm{s}^{-1}$ and 10^{-6}, respectively, one obtains that the minimum detectable fraction of molecules excited above $\kappa' h\nu_{CO_2}$ is 10^{-7}. The CO_2 induced vibrational distribution of CrO_2Cl_2 is unknown, however a value of 10^{-7} for the fraction of ground state molecules which have absorbed more than 20 CO_2 photons does not seem implausible.

Equations (9) and (17) predict long radiative lifetimes for the emitting molecules under collisionless conditions. Indeed, 60 μs CO_2 laser induced emission signals have been detected from 1 mTorr CrO_2Cl_2 samples, much longer than the roughly 1 μs[16] decay times of optically excited CrO_2Cl_2 molecules. If the induced visible emission is observed from high pressure samples, however, a rapid vibrational thermalization follows the excitation pulse, and the rate of photon emission is then given by[9]

$$I_{\mathrm{th}}=N_0\gamma_S\, e^{-E_{SG}/kT}\ , \tag{26}$$

where T is determined by the average number $\langle n\rangle$ of CO_2 photons absorbed per molecule. A collisional induced quenching has been observed for high pressure (>1 Torr) of F_2CO and CrO_2Cl_2 samples. In terms of the IER theory quenching may occur only through the disappearance of the highly vibrationally excited molecules. The following processes may account for the observed quenching.

(a) An initial nonthermal vibrational distribution is established following the CO_2 laser pulse. The emission intensity characterizing this distribution is determined by Eq. (22). If this intensity is higher than the thermal emission intensity I_{th} determined by Eq. (26), a decay of the initial intensity toward I_{th} will be observed. This decay will be determined by the thermalization time of the system.

(b) A vibrational temperature is established during or following the CO_2 excitation process. The initial emission is determined by Eq. (26), in which T is replaced by a vibrational temperature T_v. Due to the equilibration of the vibrational excitation with the rotational and translational degrees of freedom, T_v is cooled. Consequently, the emission decays towards a new value determined by the new temperature T_c common to all degrees of freedom. The difference between T_v and T_c will be significant provided that the vibrational heat capacity is equal to or less than the sum of the rotational and translational heat capacities.

(c) Once the temperature T_c is established, further cooling of the system proceeds only through thermal conductivity or infrared emission, with thermalization times of a few milliseconds. Unimolecular or bimolecular reactive channels could account for observed shorter lifetimes of the emission signals.

An expression for the fluorescence intensity from MP excited vibrational distributions of triplet biacetyl molecules is obtained by replacing G by T and N_0 by N_T^0 in Eq. (25). Since N_T^0, the number of triplet molecules prepared by the optical pulse is unknown, it is impossible to estimate the rate of the induced emission in the fluorescence region. Only a small fraction of the biacetyl molecules is trapped in the triplet state. Typical values of N_T^0 in the present experiment are therefore much smaller than the value 10^{13} assigned previously to N_0 of the chromyl chloride system. Despite the low values of N_T^0, the detection of the fluorescence signals in this experiment is qualitatively explained in terms of the relatively high values of $(\rho_S/\rho_T)_0\sim 10^{-2}$ and the high value of $\sum_{n=\kappa'}^{\infty}p(n)\sim 0.5$ achieved by the IR excitation.

ACKNOWLEDGMENT

This work was supported by the office of Naval Research (contract N0014-78-C-0531). One of us (I.B.) is indebted to Professor J. Jortner for helpful discussions.

[1]J. G. Black, E. Yablonovitch, N. Bloembergen, and S. Mukamel, Phys. Rev. Lett. **38**, 1131 (1977).
[2]See for example, C. D. Cantrell, S. M. Freund, and J. L. Lyman, in *Laser Handbook*, edited by M. Stich (North Holland, New York, 1973), Vol. 4.
[3]Z. Karny, A. Gupta, R. N. Zare, S. T. Lin, and A. M. Ronn, Chem. Phys. **37**, 15 (1979).
[4]J. W. Hudgens, J. L. Durant, D. J. Boagan, and R. A. Coveleskie, J. Chem. Phys. **70**, 5906 (1979).
[5]Y. Haas and G. Yahav, Chem. Phys. Lett. **48**, 63 (1977).
[6]I. Burak, J. Tsao, Y. Prior, and E. Yablonovitch, Chem. Phys. Lett. **68**, 31 (1979).
[7]R. Van der Werf and J. Kommandeur, Chem. Phys. **16**, 125 (1976).
[8]F. B. Wampler and R. C. Oldenberg, Int. J. Chem. Kinet. **10**, 1225 (1978).
[9]I. Burak, T. J. Quelly, and J. I. Steinfeld, J. Chem. Phys. **70**, 334 (1979).
[10]A. Nitzan and J. Jortner, Chem. Phys. Lett. **60**, 1 (1979).
[11]A. Nitzan and J. Jortner, J. Chem. Phys. **71**, 3524 (1979).
[12]R. Van der Werf, D. Zevenhuijzen and J. Jortner, Chem. Phys. **27**, 319 (1978).
[13]E. Lahmani, A. Tramer, and C. Tric, J. Chem. Phys. **60**, 4431 (1974).
[14]H. S. Kowk and E. Yablonovitch, Rev. Sci. Instrum. **46**, 814 (1975).
[15]J. W. Sidman and D. S. McClure, J. Am. Chem. Soc. **77**, 6471 (1955).
[16]J. R. McDonald, Chem. Phys. **9**, 423 (1975).